



Critical Evaluation of Multifunctional Betaxolol Hydrochloride Nanoformulations for Effective Sustained Intraocular Pressure Reduction

Jie Hu ^{1,*}, Huihui Li ^{1,*}, Yingshan Zhao¹, Yuancheng Ke¹, Ilva D Rupenthal², Hanyu Liu¹, Jinghua Ye¹, Xinyue Han¹, Fan Yang¹, Wei Li³, Huaqing Lin¹, Dongzhi Hou ¹

¹Guangdong Provincial Key Laboratory of Advanced Drug Delivery Systems and Guangdong Provincial Engineering Center of Topical Precise Drug Delivery System, College of Pharmacy, Guangdong Pharmaceutical University, Guangzhou, Guangdong, People's Republic of China; ²Buchanan Ocular Therapeutics Unit, Department of Ophthalmology, New Zealand National Eye Centre, Faculty of Medical and Health Sciences, University of Auckland, Auckland, 1142, New Zealand; ³Guangzhou Institute for Drug Control, Guangzhou, Guangdong, People's Republic of China

*These authors contributed equally to this work

Correspondence: Huaqing Lin; Dongzhi Hou, Guangdong Pharmaceutical University, Guangzhou Higher Education Mega Center, 280 Wai Huan Dong Road, Guangzhou, People's Republic of China, Tel +86 180 2631 2508, Fax +86 20 3935 2117, Email huaqing_@163.net; houdongzhi406@163.com

Introduction: Glaucoma is a chronic disease that requires long-term adherence to treatment. Topical application of conventional eye drops results in substantial drug loss due to rapid tear turnover, with poor drug bioavailability being a major challenge for efficient glaucoma treatment. We aimed to prepare the anti-glaucoma drug betaxolol hydrochloride (BH) as a novel nano-delivery system that prolonged the retention time at the ocular surface and improved bioavailability.

Methods: We constructed multifunctional nanoparticles (MMt-BH-HA/CS-ED NPs) by ion cross-linking-solvent evaporation method. The particle size, zeta potential, encapsulation efficiency and drug loading of MMt-BH-HA/CS-ED NPs were physicochemically characterized. The structure of the preparations was characterized by microscopic techniques of SEM, TEM, XPS, XRD, FTIR and TGA, and evaluated for their in vitro release performance as well as adhesion properties. Its safety was investigated using irritation assays of hemolysis experiment, Draize test and histopathology examination. Precorneal retention was examined by in vivo fluorescence tracer method and pharmacokinetics in tear fluid was studied. A model of high IOP successfully induced by injection of compound carbomer solution was used to assess the IOP-lowering efficacy of the formulation, and it was proposed that micro-interactions between the formulation and the tear film would be used to analyze the behavior at the ocular surface.

Results: The positively charged MMt-BH-HA/CS-ED NPs were successfully prepared with good two-step release properties, higher viscosity, and slower pre-corneal diffusion rate along with longer precorneal retention time compared to BH solution. The micro-interactions between nanoparticles and tear film converted the drug clearance from being controlled by fast aqueous layer turnover to slow mucin layer turnover, resulting in higher drug concentration on the ocular surface, providing more durable and stable IOP-lowering efficacy.

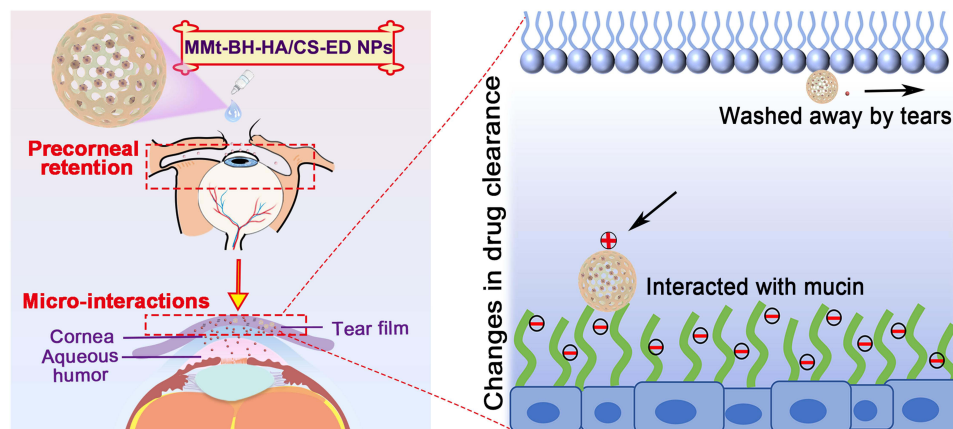
Conclusion: The novel multifunctional MMt-BH-HA/CS-ED NPs can effectively reduce IOP and are suitable for the treatment of chronic disease glaucoma.

Keywords: glaucoma, nanoparticles, betaxolol hydrochloride, BH, precorneal retention, micro-interactions

Introduction

Glaucoma is described as a group of degenerative diseases of the optic nerve,¹ often associated with pathologically elevated intraocular pressure (IOP) and characterized by progressive loss of retinal ganglion cells and irreversible loss of visual field.² It has been called the “silent thief of vision” as glaucoma shows no obvious signs or symptoms in its early stages and is only felt when vision is severely impaired,^{3,4} making it the leading cause of irreversible blindness in the world.¹ Currently, high IOP is recognized as the most important risk factor for the development of glaucoma with the risk increasing

Graphical Abstract



by 12% for every 1 mmHg increase in IOP.⁵ Lowering IOP is currently the only proven effective strategy for the treatment of glaucoma.⁶ Topical application of drugs that reduce aqueous humor production and/or increase aqueous humor outflow via the trabecular meshwork and Schlemmer's canal (eg, beta-blockers, carbonic anhydrase inhibitors, prostaglandin analogs, sympathomimetics and pupil constrictors) is the primary treatment for glaucoma.⁷ Betaxolol hydrochloride (BH) is a selective β_1 -receptor antagonist that reduces aqueous humor production by acting on β_1 -receptors to inhibit the production of cyclic adenosine monophosphate (cAMP).⁸ Compared with non-selective β -receptor antagonists such as timolol, BH results in fewer systemic side effects and has additional neuroprotective effects.⁹

Solution eye drops are most commonly used for the management of eye disorders, due to their non-invasive and rapid effect as well as their ease of administration.¹⁰ However, the unique physiological defensive mechanisms of the eye such as reflex tearing and nasolacrimal drainage, as well as the tear film and corneal barriers,^{11,12} result in less than 5% of the pharmaceuticals applied via eye drops being delivered into the anterior chamber.¹³ For this reason, frequent dosing is required to achieve the desired therapeutic response, which, however, greatly reduces patient compliance. Data suggested that patients' adherence to eye drop administration was less than 50%.¹⁴ Additionally, frequent eye drop administration throughout the day tends to cause IOP fluctuations.

Owing to the constraints above, there is an urgent need for more patient-friendly and long-acting delivery systems to improve drug bioavailability and efficacy. Indeed, nanoparticles have recently been developed to improve bioavailability and maintain long-lasting antiglaucoma efficacy.^{15–17} Nano-delivery systems are of increasing interest for ophthalmic applications due to their many advantages: Firstly, most nanocarriers are highly biocompatible.^{18,19} Secondly, they can be surface modified for tissue targeting and reduced systemic toxicity. Moreover, due to their small particle size, they may overcome most of the ocular barriers limiting drug transport into the anterior chamber. Finally, recent efforts have been focused on the development of mucoadhesive nanocarriers to enhance drug retention on the ocular surface.^{20,21}

Biopolymers have a number of beneficial inherent properties for topical ocular drug delivery, including mucoadhesive properties. Hyaluronic acid (HA), a linear anionic polysaccharide polymer with excellent biodegradability, biocompatibility, and bioadhesion,²² has attracted more attention in ocular drug delivery because it is a natural component in the vitreous body and aqueous humor.^{23,24} Particularly, HA can interact with CD44 receptors on corneal epithelial cells to achieve drug-specific binding.²⁵ Chitosan, a natural cationic polymer with good biocompatibility, biodegradability, and bioadhesion,²⁶ has a high affinity for negatively charged mucins and the glycocalyx.²⁷ In addition, cationic chitosan enables reversible loosening of tight junctions between corneal epithelial cells and thus facilitates drug penetration.²⁸ Based on these properties, negatively charged HA was cross-linked with positively charged CS to form a nano-delivery system.^{29,30} It has been reported that chitosan nanoparticles loaded with BH can prolong the retention time in the cornea, enhancing the ocular delivery of the drug.²⁰ However, there may be a drawback of drug leakage due to the good water solubility of BH.

To further improve drug encapsulation and prevent drug leakage,^{31,32} we investigated ionic crosslinking-solvent volatilization. Firstly, cationic BH was complexed with nano-clay montmorillonite to achieve sustained drug release. Montmorillonite (MMt) is a porous layered silicate consisting of two silica-oxygen tetrahedra with a layer of aluminum-oxygen octahedra sandwiched in-between,³⁰ resulting in a large surface area, excellent adsorption and ion exchange capacity, and good biocompatibility.³³ The formed MMt-BH complex was loaded into the prepared HA/CS NPs. Finally, NPs were coated with cationic Eudragit RS (ED), a water-insoluble film-forming material composed of methyl methacrylate, ethyl acrylate and trimethylamine ethyl methacrylate (molar ratio 1:2:0.1) that dissolves when exposed to water to form channels for drug release.³⁴ Due to ED's cationic nature and water absorption swelling property, it participates in micro-interactions with the ocular surface resulting in prolonged precorneal retention. It has been shown that the hydrophilic glycocalyx of negatively charged mucins in the tear film can form a discontinuous layer of hydrogel-type network structure, which is helpful in interacting with positively charged agents.^{35,36}

In the present study, the multifunctional MMt-BH-HA/CS-ED NPs were developed, and the physicochemical properties including osmotic pressure, pH, particle size, zeta potential, encapsulation rate, and drug loading were characterized. Rheology, surface tension, and contact angle were used to evaluate the viscosity and spreadability of the NPs on the ocular surface. Erythrocyte hemolysis, histopathology, and a Draize assay were performed to assess the potential irritation. Finally, micro-interactions between the formulation and the tear film mucins were analyzed to determine the precorneal retention, before evaluating the tear film pharmacokinetics and in vivo pharmacodynamics of the formulation. Such micro-interactions occurring at the ocular surface have been limitedly studied. This study innovatively advocates the use of micro-interactions between mucins and nano-delivery systems in the analysis of in vivo behavior in glaucoma treatment, which may provide good ideas for the design of ocular mucosal drug delivery systems and their behavior at the ocular surface.

Materials and Methods

Preparation of Nanoparticles

Acid-MMt was synthesized according to our previous studies to increase the surface area and cation exchange capacity.³⁷ Subsequently, MMt was acidified in 5% H₂SO₄ for 0.5 h at 70°C, and was then intercalated with BH to form a MMt-BH complex. As shown in Figure 1, MMt-BH-HA/CS-ED NPs were prepared by ion cross-linking-solvent evaporation method.^{29,32} Briefly, 10 mg of chitosan (0.5 mg/mL) in 0.2% (v/v) acetic acid that pH was adjusted to 5, were added the 5 mL of HA solution (2 mg/mL) under magnetic stirring (RCT Magnetic Stirrer, IKA Company, Germany) at 900 rpm for 30 min. In order to encapsulate the drug, MMt-BH or free BH was added to the HA solution before cross-linking with CS. Afterward, 100 mg Poloxamer 188 was added under stirring for 5 min. Subsequently, 10 mg/mL ED ethanol solution was dropped into the external aqueous phase and an ice bath ultrasound (JY92-II Ultrasound Cell Disintegrator, Shanghai Xiren Instrument Co., Ltd) was performed immediately for 5 min. Later, the formed emulsion was stirred at room temperature for 2 h to remove the organic solvent. The final MMt-BH-HA/CS-ED NPs suspension was stored at 4°C.

Physicochemical Characterization of Nanoparticles

Osmotic Pressure and pH Measurements

Mannitol (4%) was added as an osmolarity regulator and the osmotic pressure was measured with an osmometer (Osmomat Basic 3000, GonotecGmBTH, Germany). The pH was measured using a pH meter (PHS-3C, INESA Scientific Instrument Co., Ltd). Both osmotic pressure and pH were measured three times in parallel and averaged.

Particle Size and Zeta Potential Detection

The hydrodynamic diameter, polydispersity index (PDI) and zeta potential of the nanosuspensions were determined using dynamic light scattering and electrophoretic light scattering (Delsa Nano C, Beckman Coulter, Brea, CA, USA). Before the measurements, the samples were appropriately diluted with deionized water. All experiments were conducted in triplicate at room temperature.

The Examination of Drug Loading and Encapsulation Efficiency

Drug loading (DL%) and encapsulation efficiency (EE%) were determined by the dynamic dialysis method. A pre-processed dialysis bag (MW 8000–14,000 Da) containing 4 mL of nanoparticles was immersed in a beaker with 100 mL

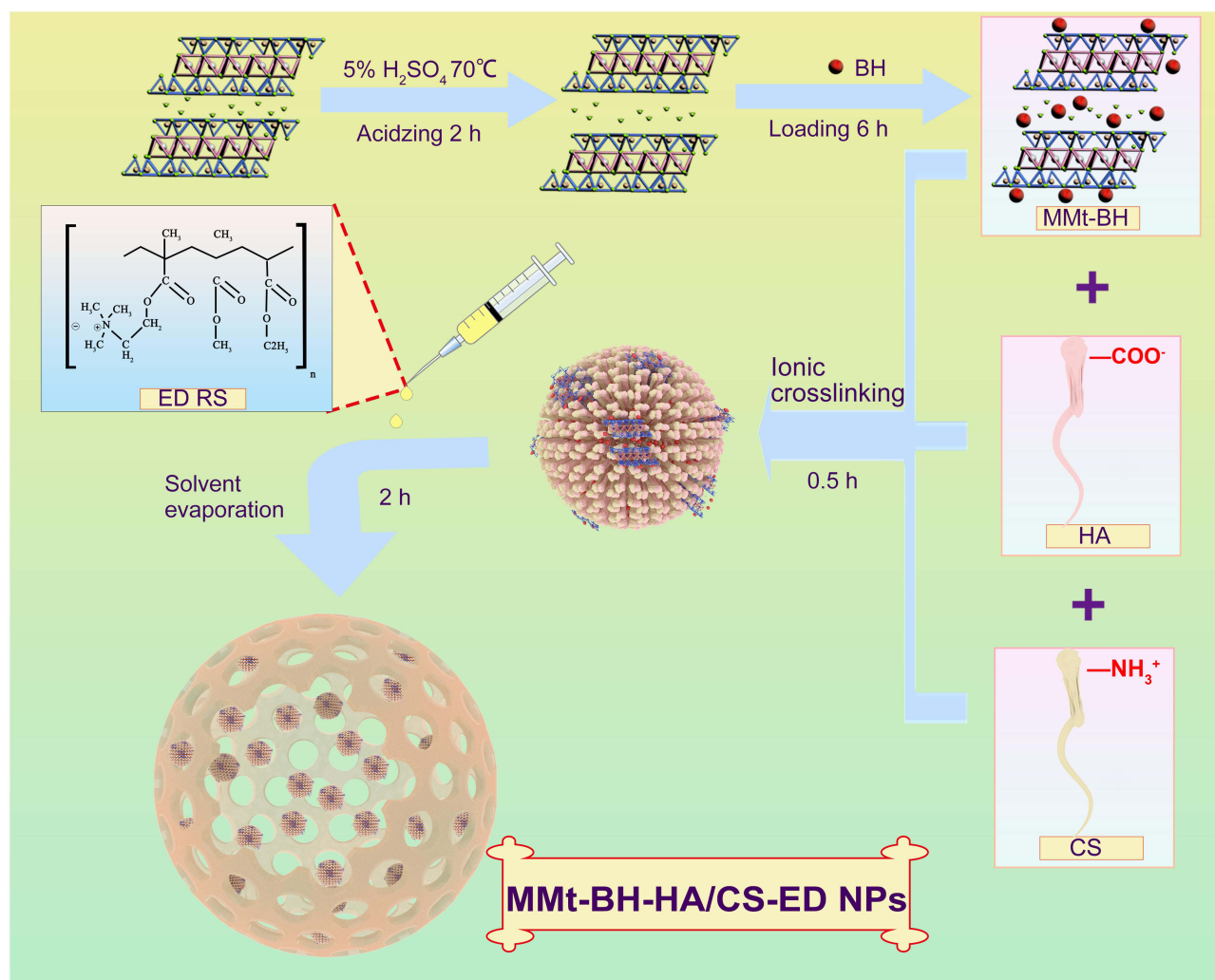


Figure 1 Schematic illustration of the preparation of multifunctional MMT-BH-HA/CS-ED NPs. The structure of montmorillonite was derived from published studies by our group.⁵¹

of deionized water for 2 h at 120 rpm and 34°C. The absorbance of free BH was measured at 273 nm by UV-Vis spectrophotometer (UV-1800; Shanghai mapada Instruments Co., Ltd, China) after filtering the solution through a 0.22 μm filter. Next, ultrasonic demulsification of nanoparticles in 10 mL methanolic hydrochloric acid solution (v:v=9:1) was performed to extract the encapsulated BH. Each experiment was performed three times. DL% and EE% were calculated according to the following equations:

$$DL(\%) = \frac{W_2 - W_0}{W} \times 100$$

$$EE(\%) = \frac{W_1 - W_0}{W_1} \times 100$$

Where W_0 is the amount of drug that is not encapsulated within the nanoparticles, W_1 is the total amount of drug added during preparation, W_2 is the total amount of drug after demulsification, W is the total mass of the nanoparticles.

Structural Characterization of Nanoparticles

Morphology

The shape and surface characteristics were observed by scanning electron microscopy (SEM, Sigma 300, Carl Zeiss, Germany) using the gold spraying technology. The internal nanoparticle morphology was assessed by transmission

electron microscopy (TEM, Philips TECNAI10, Holland) using negative staining method. To prevent particles stacking from affecting morphology, the preparations were diluted to an appropriate multiple prior to observation.

X-Ray Photoelectron Spectroscopy

In order to characterize the surface composition of the prepared nanoparticles, an X-ray photoelectron spectrometer (XPS, Thermo Fisher Scientific, UK) equipped with a monochrome Al-K α X-ray source (excitation energy: 1468.6 eV) was utilized. Samples were pressed into thin slices and placed in the sample chamber for vacuum treatment until the pressure was below 5×10^{-8} mbar. Then, the spectrum was collected from 0 to 1350 eV with a wide sweep of 100 eV and a single element of 30 eV. All binding energies were calibrated with the C1s peak at 284.8 eV.

X-Ray Diffraction Spectroscopy

X-ray diffraction (XRD) was performed on pure BH, acid-MMt, MMt-BH and MMt-BH-HA/CS-ED NPs using an X-ray diffractometer (Rigaku MiniFlex 600, Japan) with Ni filtered at a generator voltage of 40 kV and tube current of 40 mA utilizing Cu K α radiation. Samples were placed in the sample holder and scanned at a rate of 1° min^{-1} from 3° to 80° .

Fourier Transform Infrared Spectroscopy

Samples of 1 mg were mixed with 100 mg KBr and ground evenly in an agate mortar. Samples were pressed by a tablet press into split-free flakes and then scanned from 400 to 4000 cm^{-1} using a Fourier transform infrared spectrometer (FTIR, TENSOR27, Bruker Company, Germany).

Thermogravimetric Analysis

A differential scanning calorimetry (DSC) method was used to observe the phase transformation process of each sample powder by thermogravimetric analysis. This experiment was carried out using a simultaneous thermal analyser (STA 409 PC LUXX, Netzsch Company, Germany) in a nitrogen flow of $60 \text{ mL} \cdot \text{min}^{-1}$ with a ramp-up rate of $10^\circ\text{C} \cdot \text{min}^{-1}$ from 30°C to 1000°C .

Viscosity and Spreadability

Rheological Properties

A rheometer with the parallel plate system was used to complete the viscosity measurement. The viscosity was recorded using a parallel plate system (Anton Paar Physica MCR301, Austria) at a shear rate from 1 to 200 s^{-1} at 34°C to simulate the flow of MMt-BH-HA/CS-ED NPs on the ocular surface after blinking. Rheology curves were fitted by the Ostwald-de Waele power law equation:

$$\tau = K \dot{\gamma}^n$$

Where K is the viscosity coefficient and n is the non-Newtonian index of the fluid.

Surface Tension and Contact Angle

The surface tension and contact angle of the BH solution and MMt-BH-HA/CS-ED NPs were measured by the pendant drop method.³⁸ The eyeballs of healthy New Zealand rabbits stored in saline were placed on the sample table with the corneal facing up, and the preparations were dropped slowly from a 1 mL syringe with images taken perpendicular to the syringe. The images of the moment the droplet left the needle were taken, and the system would record the surface tension of the droplet at that moment. Each image was subsequently analyzed to obtain the contact angle by measuring the angle between the corneal surface and droplet tangent. All experiments were carried out in triplicate using an optical contact angle instrument (SDC-100, Dingsheng, China).

In vitro Release Studies

The dynamic dialysis method was used to study the release behavior of the preparation in vitro. Fresh simulated tear fluid (STF, pH 7.4) composed of NaCl 0.680 g, NaHCO₃ 0.220 g, KCl 0.140 g, and CaCl₂ 0.008 g in 100 mL of deionized water was prepared as release medium.¹⁷ Then, 4 mL of BH solution (2.8 mg/mL) or the nanosuspension (2.8 mg/mL for 15.92% drug loading) was placed into the pre-treated dialysis bag (MW 8000–14,000 Da) and immersed into a beaker

containing 100 mL STF, before placing the entire system in an air-bath thermostatic oscillator at 120 rpm and 34°C. At pre-determined time intervals, 5 mL of the release medium was collected and replaced with the same amount of fresh STF to maintain sink condition. The collected samples were filtered through a 0.22 µm filter and the drug content was measured at 273 nm using a UV-Vis spectrophotometer (UV-1800; Shanghai mapada Instruments Co., Ltd, China).

Irritation Potential

Hemolysis Experiment

To assess the possible irritation of MMt-BH-HA/CS-ED NPs, the hemolysis assay was performed to verify it at the cellular level. Firstly, red blood cells (RBC) were obtained from 2 mL heparinized fresh rabbit blood and diluted with 20 mL PBS. Then, 0.8 mL of NPs were added into 0.2 mL of RBC suspension and cultured at 37°C for 4 h. After incubation, samples were centrifuged at 10,000 rpm for 5 min and the absorbance of 100 µL supernatant placed in a 96-well plate, was determined at 570 nm using a microplate reader (MultiskanFC, Thermo Fisher Scientific, China). PBS solution was used as the negative control, and distilled water as the positive control, with the hemolysis rate (HR%) determined as follows:

$$HR(\%) = \frac{A_2 - A_0}{A_1 - A_0} \times 100$$

Where A_2 is the absorbance of the tested formulation group, A_1 is the absorbance of the negative, and A_0 is the absorbance of the positive control.

Draize Test

Six healthy New Zealand white rabbits were randomly divided into two groups: BH solution and MMt-BH-HA/CS-ED NPs. A volume of 100 µL of the sample was applied to the left eye of each rabbit with the right eye receiving an equal volume of saline. The eyelids were gently closed for about 10s to prevent spillage. In the short-term test, each group received only one eye drop administration, while in the long-term test, rabbits were treated three times a day for nine days. The ocular response (edema, secretions, cornea lesions, iris and conjunctival congestion) of each animal was observed at 1, 24, 48 and 72 h after administration for the short-term test and prior to daily administration for the long-term test and scored according to a previously published scoring system.³⁹

Histopathology Examination

Histopathological analysis was performed on ocular tissues after the long-term irritation. Briefly, excised tissues were immersed in 10% formalin, dehydrated in ethanol, embedded in molten paraffin and cut into thin slices for Hematoxylin and Eosin (H&E) staining. Images were acquired using a light microscope (BK6000, Chongqing Optec Instrument Co., Ltd.).

In vivo Animal Experiments

New Zealand white rabbits of either sex without ocular abnormalities (SCXK 2016-0041), weighing 1.5–2.0 kg, were purchased from the Southern Medical University Laboratory Animal Center (Guangzhou, China), and all animal experiments were conducted in accordance with the “Guiding Principles in the Care and Use of Animals (China, GB/T35892-2018)” and were approved by the Institutional Animal Care and Use Committee of Guangdong Pharmaceutical University (Acceptance No: gdpulou2021196).

Precorneal Retention Evaluation

A fluorescence tracing method was used to assess the precorneal retention time of the NPs on the rabbit ocular surface.⁴⁰ Six healthy New Zealand white rabbits were selected and randomly divided into two groups. BH replaced by sodium fluorescein loading was performed as described in Physicochemical Characterization of Nanoparticles. Then, 100 µL of formulation (sodium fluorescein solution and MMt-fluorescein-HA/CS-ED NPs) was applied into the conjunctival sac of rabbit eyes before gently closing the eyes for 10 s. The changes in fluorescence intensity were recorded at regular intervals using a slit lamp under cobalt blue light (YZ5S, Liuliu Vision Technology Co., Ltd.).

Tear Drug Pharmacokinetic Studies

Tear drug pharmacokinetics was determined based on previous studies with minor modifications.⁴¹ Six healthy New Zealand white rabbits were randomly divided into two groups (BH solution and MMt-BH-HA/CS-ED NPs). The left eye of each rabbit received 100 μ L saline (control) while the right eye received an equal volume of the test formulation. The nasolacrimal duct was gently pressed to reduce significant loss. At specific time-points, pre-weighed strips of filter paper were lightly placed under the upper eyelids and the amount of tear sample collected was determined by mixing test strips with 70 μ L methyl alcohol, vortexing for 2 min and centrifuging at 15,000 rpm for 10 min. Finally, 20 μ L of supernatant was quantified for drug content using HPLC (LC-20AT, Shimadzu, Japan).⁴² The drug concentration of BH was measured using an Inertsil ODS-C18 column with a mixture of acetonitrile and 0.2% triethylamine (v:v=3:7) as the mobile phase at a detection wavelength of 273 nm. Finally, the concentration of BH was calculated with a standard curve ($Y = 0.0069X - 0.00993$, $R^2 = 0.9990$, X was the concentration of BH in aqueous solution ranging from 1 to 300 μ g/mL, Y was the peak areas of chromatography).

Pharmacodynamic Assessment

Rabbits were checked for three consecutive days prior to the start of the study to ensure that the IOP was within the normal range from 10 to 21 mmHg.³ In order to induce ocular hypertension, 0.1 mL of aqueous humor was withdrawn after anesthesia, and the same volume of compound carbomer including 0.3% carbomer and 0.025% dexamethasone was injected into the anterior chamber.⁴² After 7 days, rabbits with an IOP >22 mmHg were selected and randomly divided into three test groups (saline, BH solution and MMt-BH-HA/CS-ED NPs). A volume of 100 μ L of saline, BH solution and MMt-BH-HA/CS-ED NPs was instilled, respectively. The IOP was measured three times using an iCare tonometer (Tonovet plus, iCare, Finland) at specific point time under the same environmental conditions.

Statistical Analysis

Experimental results were uniformly expressed as mean \pm standard deviation, and Origin2022 software (OriginLab, USA) was used for significant difference analysis on independent sample *t*-test and one-way ANOVA. A comparison of $p < 0.05$ was considered statistically significant and marked with an asterisk.

Results and Discussion

Preparation of Nanoparticles

MMt-BH-HA/CS-ED NPs were successfully prepared by the ionic cross-linking-solvent evaporation method and resulted in a light blue formulation with a Tyndall effect. The relevant physicochemical properties of the NPs are summarized in Table 1. The average NPs size was 778.90 ± 60.88 nm with a narrow PDI, which would reduce discomforts such as blinking and thus tear production caused by the large particles (>10 μ m). The positive zeta potential of 21.28 ± 1.11 mV prevented particle aggregation due to repulsion, and facilitated better micro-interactions with negatively charged tear film mucins as further discussed below. The pH and osmotic pressure of the formulation were 6.94 ± 0.17 and 301.33 ± 3.86 mOsmol/kg, respectively, with both being within the optimal range for eye drops (pH 6.8 to 8.2 and 270 to 315 mOsmol/kg, respectively).⁴³ The EE% and DL% were $85.40 \pm 0.20\%$ and $15.92 \pm 0.26\%$, indicating that the NPs were able to load more drug than our previously prepared single polymer NPs (CS NPs⁴⁴ and ED NPs).³²

Table 1 Physicochemical Properties of MMT-BH-HA/CS-ED NPs (Mean \pm SD, n = 3)

Particle Size (nm)	PDI	Zeta Potential (mV)	pH	Osmolarity (mOsmol/kg)
778.90 \pm 60.88	0.327 \pm 0.021	21.28 \pm 1.11	6.94 \pm 0.17	301.33 \pm 3.86

Structural Characterization of Nanoparticles

Morphological Observations

SEM micrographs (Figure 2A left) showed that NPs were spherical with a smooth surface and a particle size of around 750 nm, which is consistent with the particle size results (Table 1). Similarly, TEM micrographs (Figure 2A right) revealed that the NPs had a core-shell structure with a dark inner and a light outer ring, suggesting the formation of HA/CS drug-loaded NPs with an ED outer layer.

X-Ray Photoelectron Spectroscopy

XPS is a powerful tool for analyzing the elemental composition of the NP surface. XPS results revealed that BH was loaded into the MMt and formed MMt-BH-HA/CS-ED NPs (Figure 2B). The XPS spectrum of BH showed an extremely strong N 1s peak at 402 eV with MMt-BH also having a distinct N 1s peak compared to acid-MMt, indicating that BH was successfully loaded into MMt (Figure 2C). In the Cl 2p XPS spectra, MMt-BH exhibited no characteristic peak at 197 eV, which further confirmed that BH was embedded in the MMt layer through an ion exchange mechanism (Figure 2D). In addition, weak Si 2p (Figure 2E) and Cl 2p signals in NPs were detected at 103 eV and 197 eV, suggesting that a small amount of BH and MMt-BH was adsorbed onto the surface of the NPs, while more was encapsulated internally. Most importantly, the Al 2p XPS spectra (Figure 2F) showed no signal suggesting that interactions between the various polymers and the drug had occurred.

X-Ray Diffraction Spectroscopy

XRD is a method of physical analysis that identifies the state of a sample by analyzing the intensity and shape of the peaks. Sharp, high peaks indicate a highly crystalline sample, while broad, short peaks indicate an amorphous structure. The XRD spectra of each sample are shown in Figure 2G. BH exhibited numerous distinct peaks at 5.64°, 11.24°, 13.45°, 19.95°, 23.39° and 24.2°, which suggested that the sample was in the crystalline form. Similarly, the crystalline structure of the Acid-MMt dispersion had peaks at 7.14°, 19.69° and 20.87° with a basal spacing of 1.237 nm. However, the (001) reflection of MMt-BH was shifted to 4.67° and the basal spacing was increased to 1.891 nm which was higher than that of Acid-MMt, demonstrating that BH intercalated to the MMt interlayer successfully through an ion exchange mechanism. Compared to the crystalline diffraction peaks of BH and MMt-BH, NPs revealed distinct differences, indicating an amorphous nature of the drug after encapsulation which may enhance physical stability and dissolution velocity.⁴⁵

Fourier Transforms Infrared Spectroscopy

FTIR is used to study the chemical composition and structure of samples with a disappearance or broadening of the peak as well as a change in wave number indicating the formation of a complex. As shown in Figure 2H, Acid-MMt has a stretching vibration peak of the Al-OH bond at 3614 cm⁻¹ corresponding to a bending vibration peak at 787 cm⁻¹, and a characteristic peak of adsorbed water H-O-H at 3440 cm⁻¹ corresponding to a bending vibration peak at 1640 cm⁻¹.⁴⁶ The absorption peak at 1034 cm⁻¹ is an asymmetric stretching vibration of the Si-O-Si bond. The BH spectra showed an absorption band for -OH at 3251 cm⁻¹, characteristic peaks at 2941 cm⁻¹, 2863 cm⁻¹, and 2790 cm⁻¹ attributed to alkyl stretching vibrations, and a peak at 1513 cm⁻¹ indicating the aromatic ring, which appeared in the MMt-BH pattern but not in Acid-MMt, indicating that BH was loaded into MMt. Furthermore, the disappearance of the characteristic peak of BH in NPs, such as the peak at 1247 cm⁻¹ and at 1513 cm⁻¹ representing the C-O-C stretching vibration, as well as the peak at 1034 cm⁻¹ in MMt-BH showing movement to 1099 cm⁻¹ in the NPs, suggested that both BH and MMt-BH were incorporated into the NPs.

Thermogravimetric Analysis

TGA curves for the same mass of Acid-MMt and MMt-BH showed a different total mass loss indicating successful intercalation of BH (Figure 2I). In addition, both Acid-MMt and MMt-BH showed higher final retention compared to the TGA curves of the other substances, indicating that high temperature would not destroy the lamellar structure of MMt. Mass loss of MMt-BH-HA/CS-ED NPs at 362–508°C indicated disintegration of the carrier materials, with a final ~5% residue, which could be the undecomposed MMt encapsulated in the NPs. All the above results demonstrated the

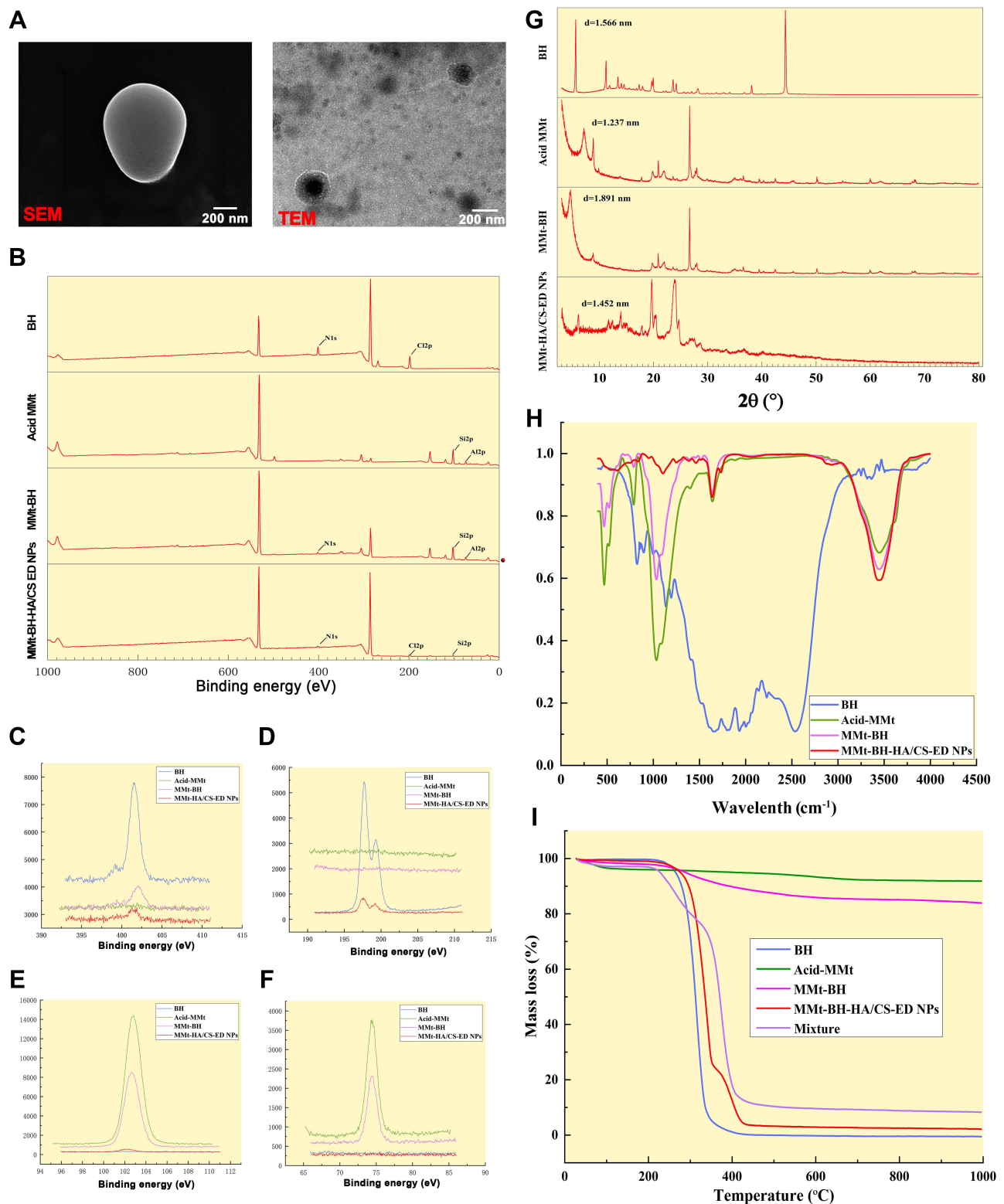


Figure 2 Characterization of MMt-BH HA/CS-ED NPs. **(A)** SEM and TEM micrographs of MMt-BH HA/CS-ED NPs. **(B)** X-ray spectra, **(C)** N 1s XPS spectra, **(D)** Cl 2p XPS spectra, **(E)** Si 2p XPS spectra, and **(F)** Al 2p spectra of BH, Acid-MMt, MMt-BH, and MMt-BH HA/CS-ED NPs. **(G)** XRD spectra. **(H)** FTIR spectra of BH, Acid-MMt, MMt-BH, and MMt-BH HA/CS-ED NPs. **(I)** TGA curves of BH, Acid-MMt, MMt-BH, MMt-BH-HA/CS-ED NPs and ED, HA and CS physical polymer mixture.

formation of MMt-BH-HA/CS-ED NPs by ionic cross-linking-solvent evaporation and the successful encapsulation of MMT-BH complexes.

Viscosity and Spreadability

Rheological Properties

Ophthalmic preparations with appropriate viscosity can prolong the precorneal retention time. The variation of the viscosity of the nanosuspension with increasing shear rate is shown in [Figure 3A](#). As can be seen, the suspension had a higher viscosity at low shear (~ 9 mPa·s) which may facilitate NPs adhesion to the ocular surface and enable better drug contact with the cornea. As the shear rate increased, the viscosity decreased, indicating that the nanosuspension was a shear-thinning pseudoplastic fluid, which was consistent with the Ostwald-de Waele power-law equation subsequently fitted ($n < 1$). As such, blinking with a shear rate of $4250\text{--}28,500\text{ s}^{-1}$,⁴⁷ would result in shear thinning of the formulation, reducing any irritation and enabling uniform distribution across the ocular surface.

Surface Tension and Contact Angle

Surface tension and contact angle are important parameters in the evaluation of liquid formulations, the former determining the degree of spreading and the latter influencing the wetting of the formulation on the ocular surface. The surface tension of human tears is $40\text{--}50$ mN/m, and liquids below this value are favorable for spreading in tears and maintaining tear film stability.⁴⁸ The surface tension of the nanosuspension (38.73 mN/m) was significantly lower ($p < 0.05$) than that of the BH solution (44.65 mN/m) and slightly lower than that of human tear, making it easier to mix with the tears and maintain good spread on the cornea ([Figure 3B](#)). Meanwhile, acceptable viscosity, as shown by the viscosity test, may improve retention, which was further supported by the spreading time on isolated cornea with the NPs having a longer spreading time compared to the BH solution. The smaller contact angle (16.70°) of the nanosuspensions is beneficial to wet the cornea and thus better spread across the ocular surface. Together, these results demonstrated that the prepared NPs have the potential to extend precorneal retention time, increasing the effective release time of the drug on the ocular surface.

In vitro Release Studies

In vitro release studies are an effective alternative method to evaluate and predict the bioavailability of formulations in vivo. [Figure 3C](#) presents the in vitro release profiles of the BH solution, BH-HA/CS-ED NPs and MMt-BH-HA/CS-ED NPs. As expected, BH was rapidly released from the solution with approximately 51% at 0.5 h and almost 100% within 2.5 h. The release of MMt-BH-HA/CS-ED NPs and BH-HA/CS-ED NPs showed a sustained fashion that they released about 32% at almost the same release rate in the first 0.5 h, followed by a slow release up to 5 h with a cumulative release of 82.23% and 93.61%, respectively, suggesting a weak burst release effect attributed to the adsorption of small drug amounts of on the NPs surface. The cumulative release amount of MMt-BH-HA/CS-ED NPs was slightly lower than that of BH-HA/CS-ED NPs after 0.5 h, which meant that the release rate of MMt-BH-HA/CS-ED NPs was slower than that of BH-HA/CS-ED NPs after 0.5 h, indicating that the MMt sandwich structure provided additional sustained release, which resulted in a significantly ($p < 0.01$) slower release of the drug. The final 5 h cumulative release amount was lower than that of the BH-HA/CS-ED NPs, which may be resulted from the adsorption of the cationic drug BH by the negatively charged laminate of the MMt and the presence of surrounding polymer molecular chains interfering with the release. The weak burst release and high cumulative release amount of MMt-BH-HA/CS-ED NPs, with their own help of superior viscosity and spread properties, will be conducive to create favorable conditions for achieving high bioavailability of NPs in vivo.

The in vitro release curves of the three formulations were fitted to various release kinetic models ([Table 2](#)). The best-fit equation models for MMt-BH-HA/CS-ED NPs and BH-HA/CS-ED NPs were first-order release kinetic equations with R^2 of 0.9988 and 0.9983, respectively. The Ritger-Peppas model equation showed n values of 0.2372 and 0.2992, respectively, both of which were less than 0.45, indicating that the BH release was according to Fick diffusion.

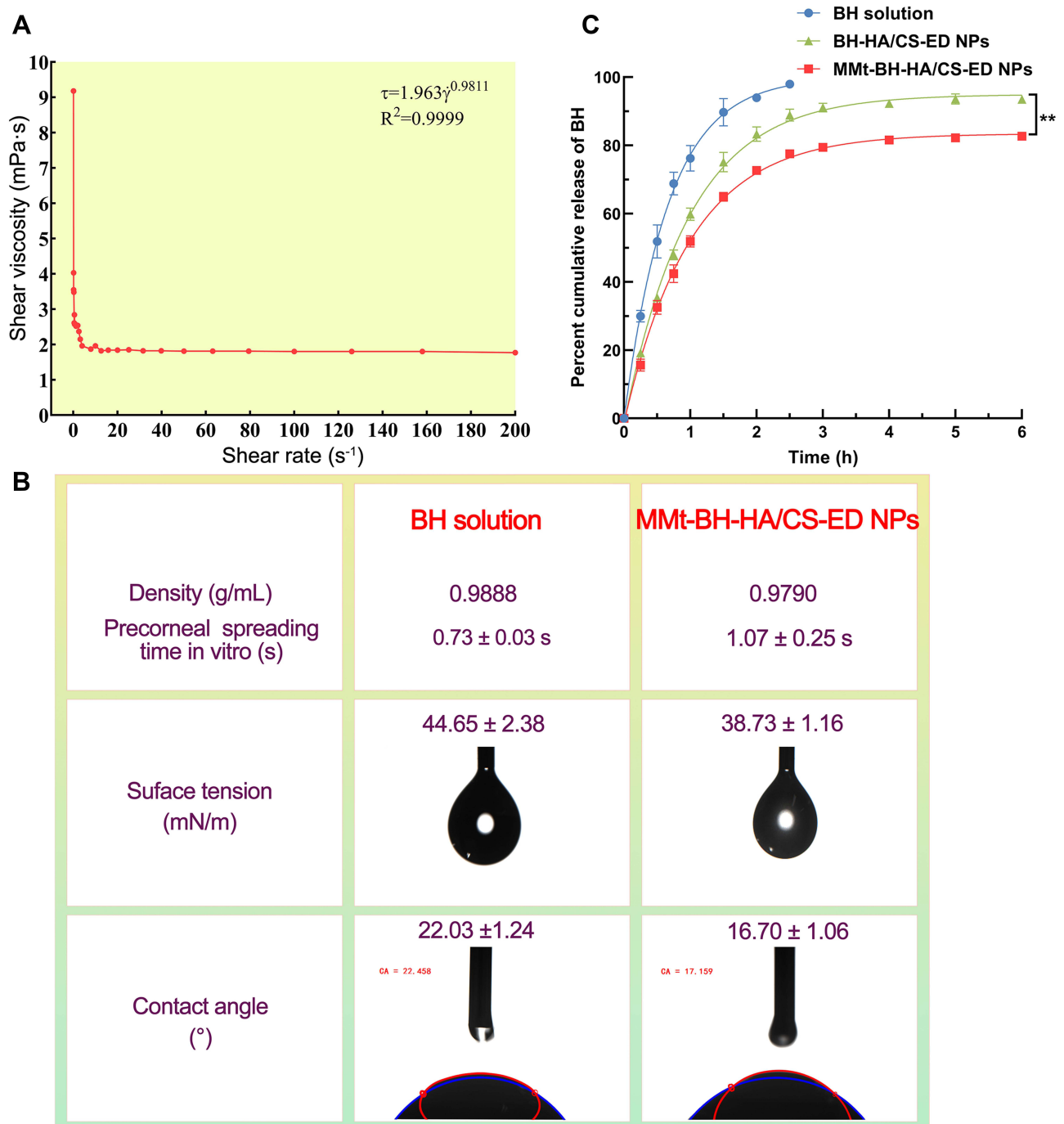


Figure 3 (A) Rheological profile of the MMt-BH-HA/CS-ED NPs. (B) Surface tension, contact angle, and vitro precorneal spreading time values of the BH solution and MMt-BH-HA/CS-ED NPs (mean ± SD, n = 3). (C) In vitro drug release profile of BH solution, BH-HA/CS-ED NPs, and MMt-BH-HA/CS-ED NPs, (mean ± SD, n = 3, **p < 0.01).

Irritation Potential

Hemolysis Experiment

Erythrocytes subjected to adverse external environmental changes will swell or even leak their contents. Therefore, there is great importance for ocular preparations to assess potential irritation by sensitive erythrocyte hemolysis. According to the Standard Practice of the American Society for Testing and Materials Designation (ASTMF-756-00), hemolysis rates above 5% are considered severely hemolytic, below 2% and in between are considered non-hemolytic and slightly hemolytic, respectively.⁴⁹ Figure 4A shows that the supernatant of the positive control group was bright red with only a small amount of precipitation at the

Table 2 Fitting Results for in vitro BH Release from MMt-BH-HA/CS-ED NPs (n = 3)

Formulations	Models	Equation	R ²
BH solution	Zero order	Q=26.1006t+35.2629	0.7684
	First order	Q=100.1165(1-e ^{-1.4750t})	0.9991
	Higuchi	Q=65.6805t ^{1/2} +3.6894	0.9632
BH-HA/CS-ED NPs	Zero order	Q=5.1907t+50.5838	0.4592
	First order	Q=94.3996(1-e ^{-1.0038t})	0.9983
	Higuchi	Q=23.9044t ^{1/2} + 29.3399	0.7019
	Ritger-Pappas	Q=59.5571t ^{0.2992}	0.8523
MMt-BH-HA/CS-ED NPs	Zero order	Q=43.9046t+4.7431	0.4878
	First order	Q=83.7642 (1-e ^{-0.9699t})	0.9988
	Higuchi	Q=21.6207t ^{1/2} +21.9146	0.7274
	Ritger-Pappas	Q=52.0017t ^{0.2372}	0.8671

bottom, indicating that the majority erythrocytes had been destroyed producing severe hemolysis, while the supernatants of the negative control and each test group were clear and intact erythrocytes were accumulated at the bottom. The hemolysis rate was calculated to be 3.02±0.07% for the BH solution and 0.45±0.55% for NPs, which was significantly less than that of the BH solution (p < 0.01), suggesting that the drug encapsulation can reduce the toxicity caused by drug aggregation, with the nano-delivery system presenting excellent biocompatibility in terms of cytotoxicity and hemolysis.

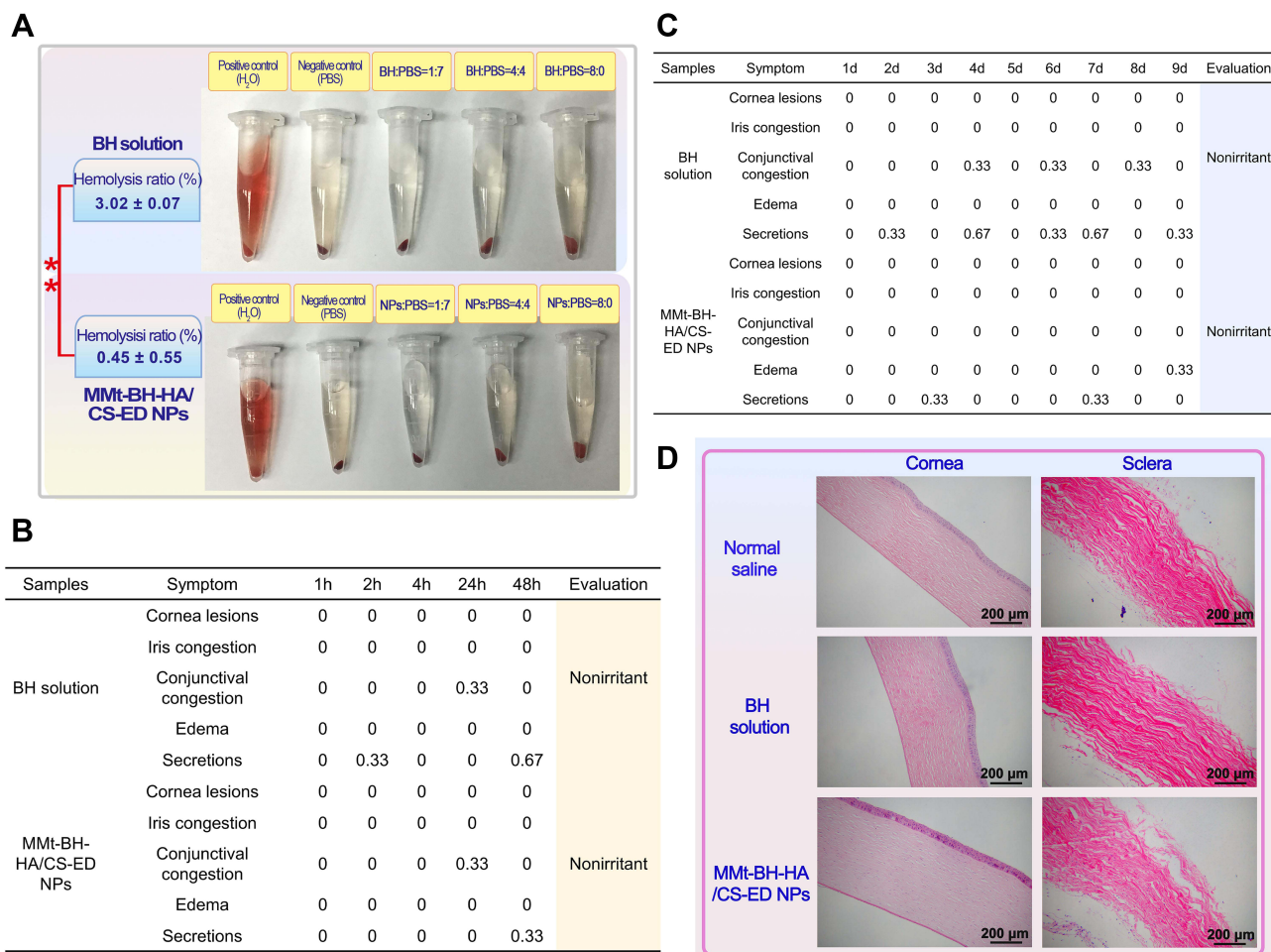


Figure 4 Ocular irritation of the BH solution and MMt-BH-HA/CS-ED NPs. (A) Hemolysis experiment results. (B) Short-term irritation score. (C) Long-term irritation score. (D) Histopathological analysis of cornea and sclera (100× magnification) after long-term irritation test.

Draize Test

Irritant substances can cause reflex blinking and increased tear secretion or even redness, accordingly reducing precorneal drug retention and potential irritation of the eyes. The Draize test scores the response of the ocular tissues to various stimuli, with a score above 3 being considered irritating. Short-term and long-term stimulation test results are shown [Figure 4B and C](#). BH solution and NPs only caused minor eye irritation such as increased secretion and conjunctival congestion with all scores lower than 3, indicating that both had little short- and long-term irritant potential. It should be noted that rabbit eyes are generally more sensitive than human eyes, thus it is reasonable to believe that MMt-BH-HA/CS-ED NPs may have good ocular tolerance in humans.

Histopathology Examination

Histological sections of the cornea and sclera after long-term administration are shown in [Figure 4D](#). There was no significant difference between the groups except for the BH solution group, which showed mild edema of the corneal epithelium. The collagenous scleral fibers were tightly arranged without inflammatory reactions. Thus, H&E staining suggested that repeated administration of MMt-BH-HA/CS-ED NPs did not damage the cornea and sclera. Combined with the results of the hemolysis and Draize tests, it was clearly demonstrated that MMt-BH-HA/CS-ED NPs may reduce the toxicity of free BH and improve the long-term treatment of glaucoma with BH.

Precorneal Retention Evaluation

To observe the precorneal retention of MMt-BH-HA/CS-ED NPs, we physically encapsulated sodium fluorescein into the NPs and used a sodium fluorescein solution as a control. As shown in [Figure 5A](#), both sodium fluorescein solution and NPs resulted in bright green fluorescence within 10 s after administration. Not surprisingly, there was a substantial loss of fluorescence in the solution group at 3 min with only faint fluorescence retained after 15 min, likely due to tear turnover and nasolacrimal drainage ([Figure 5A \(#\) and \(##\)](#)). However, MMt-fluorescein-HA/CS-ED NPs significantly increased the retention time on the ocular surface with fluorescence still observed at 50 min, with a final retention time of 85.33 ± 9.67 min, 4.6 times longer than that of the solution (18.67 ± 1.69 min). This implied that the synergistic effect of micro-interactions between positively charged MMt-BH-HA/CS-ED NPs and negatively charged tear film mucins as well as the higher viscosity contributed to the prolonged precorneal retention time.

Tear Drug Pharmacokinetic Studies

Concentration-time curves after application of the BH solution and MMt-BH-HA/CS-ED NPs are presented in [Figure 5B](#). At 5 min, the BH concentration after application of the MMt-BH-HA/CS-ED NPs ($659.34 \mu\text{g}\cdot\text{mL}^{-1}$) was 2.3 times higher than that in the BH solution group ($282.64 \mu\text{g}\cdot\text{mL}^{-1}$). It is known that tears are constantly renewed and metabolized at a rate of approximately $1.6 \mu\text{L}\cdot\text{min}^{-1}$,⁴³ resulting in the rapid elimination of the BH solution such that the drug cannot be accurately quantified after 2 h. However, BH could be consistently detected in tears up to 6 h after application of MMt-BH-HA/CS-ED NPs, which was consistent with in vitro drug released up to 6 h. The pharmacokinetic parameters were analyzed by the non-compartment model, and the excellent retention ability of MMt-BH-HA/CS-ED NPs was further confirmed by the MRT_{0-t} ([Table 3](#)). Correspondingly, the AUC_{0-t} for the NPs was also significantly higher than that of the BH solution, indicating that encapsulation significantly improves drug bioavailability. The concentration-time profiles and pharmacokinetic parameters in tears together demonstrated that the positively charged mucoadhesive nano-delivery system interacted with the negatively charged tear film mucins, which not only resulted in prolonged pre-corneal retention but also enhanced drug bioavailability as further discussed below.

Pharmacodynamic Assessment

To further validate that the proposed NPs enhance drug bioavailability, we investigated the in vivo pharmacodynamics of the BH solution and MMt-BH-HA/CS-ED NPs after a single topical application in a rabbit model of high IOP. As shown in [Figure 5C](#), the saline group (negative control) exhibited small fluctuations in IOP over the period of 12 h, which excluded the possibility of IOP-lowering effect due to rabbit self-regulation. The BH solution group (positive control) showed a good IOP-lowering effect during the first 4 h, but there was a large IOP fluctuation at 1.5 h. For the MMt-BH-

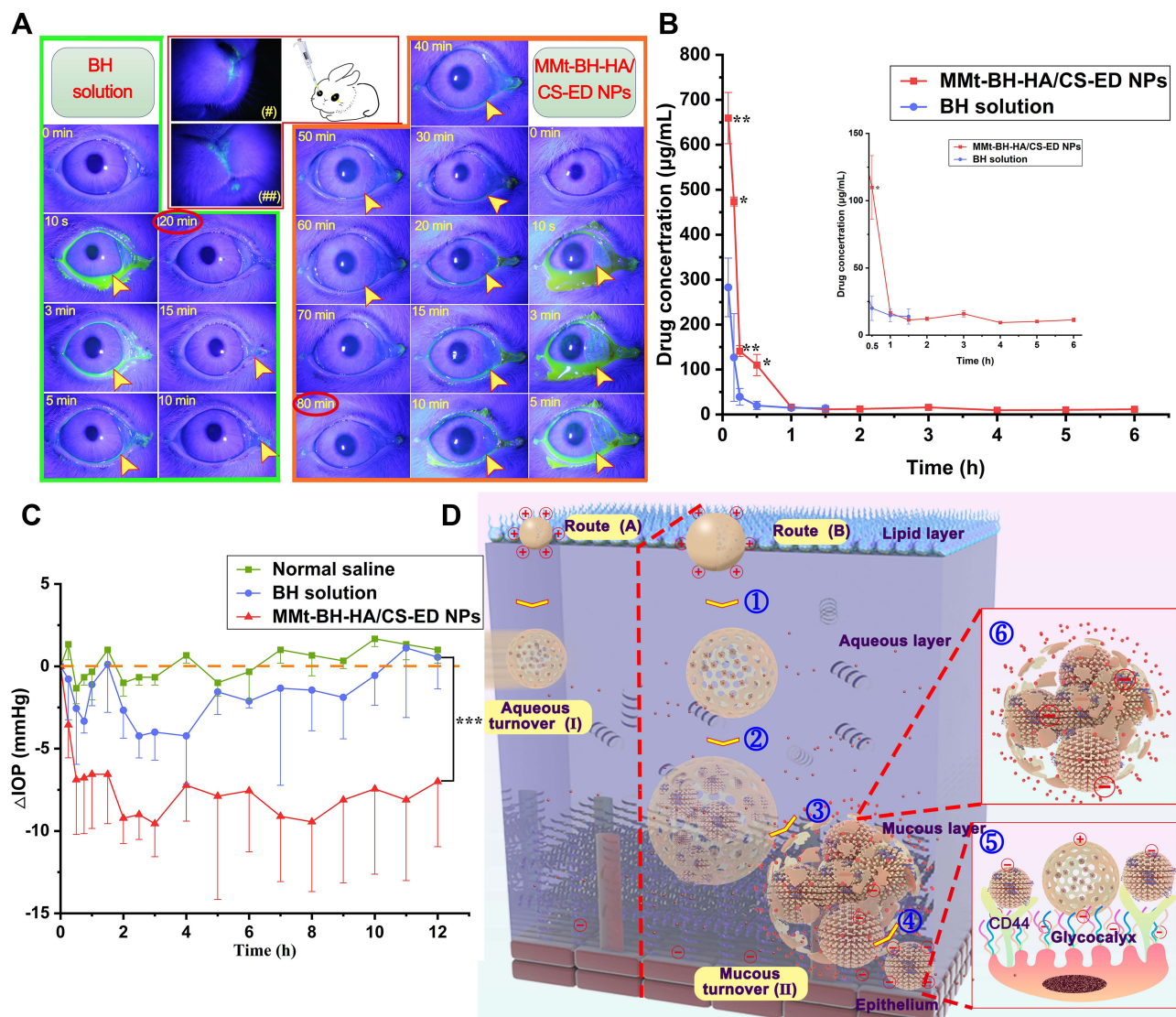


Figure 5 Precorneal retention and pharmacodynamic evaluation. **(A)** In vivo tracing of fluorescein sodium solution and MMT-fluorescein-HA/CS-ED NPs following single topical instillation, where # and ## represent loss through nasolacrimal drainage. **(B)** The concentration–time curves of BH after application of the BH solution and MMT-BH-HA/CS-ED NPs in rabbit tears (mean \pm SD, $n = 3$, * $p < 0.05$, ** $p < 0.01$). **(C)** IOP lowering effects of the BH solution and MMT-BH-HA/CS-ED NPs compared to saline (mean \pm SD, $n = 3$, *** $p < 0.001$). **(D)** Schematic diagram of micro-interactions between MMT-BH-HA/CS-ED NPs and the tear film: Route (A) suggests that MMT-BH-HA/CS-ED NPs that are too small or too large are easily washed away by the tears (I); Route (B) suggests that MMT-BH-HA/CS-ED NPs with the optimal particle size are capable of micro-interactions with negatively charged tear film mucin due to their positive surface charge, changing the drug clearance rate from tear aqueous turnover to mucous turnover (II).

HA/CS-ED NPs group (test group), the IOP-lowering effect over the 12 h period was significantly better than that of the BH solution with minimal fluctuations seen over the investigation period. It is worth noting that the IOP in the group treated with MMT-BH-HA/CS-ED NPs remained low after 12 h, while that of rabbits treated with the BH solution returned to the starting IOP value after 4 h.

Table 3 Pharmacokinetic Parameters After Application of the BH Aqueous Solution and MMT-BH-HA/CS-ED NPs

Preparations	AUC _{0-t} (mg min ⁻¹ L ⁻¹)	MRT _{0-t} (min)
BH solution	2011.28 \pm 21.59	27.18 \pm 5.44
MMt-HA/CS-ED NPs	12811.97 \pm 941.50***	66.56 \pm 1.47**

Notes: mean \pm SD, $n = 3$, * $p < 0.01$, *** $p < 0.001$.

Abbreviations: AUC, area under the curve; MRT, mean residence time.

Compared to the BH solution, MMt-BH-HA/CS-ED NPs have sustained IOP-lowering effect, which is not only connected to the extrinsic factors such as the slow released properties, suitable viscosity and prolonged precorneal retention time, but can also be attributed to intrinsic factors such as the micro-interactions between the negatively charged mucins and the positively charged NPs.^{21,35} The hydrogel-type meshwork formed by mucins in the tear film has efficiently trapped NPs of a certain size. The negatively charged polysaccharides attached to the surface of corneal epithelial cells extend into the tear film forming the glycocalyx. Figure 5D depicts the potential micro-interactions between MMt-BH-HA/CS-ED NPs and the tear film. After topical administration, MMt-BH-HA/CS-ED NPs that are too large or too small are easily washed away by the tears (I, Route A),³⁶ whereas MMt-BH-HA/CS-ED NPs of optimal particle size were capable of micro-interactions with negatively charged mucins in tears due to their positive charge, changing the drug clearance from tear aqueous turnover to mucous turnover (II), thus prolonging their precorneal retention time (route B). For route B, firstly, the ED shell absorbed water with the swelling resulting in pore formation allowing water and some cations present in the tears to enter the inner core. The drug on/in the MMt was then separated by ion exchange and released from the pores together with the drug encapsulated in the inner HA-CS core (step ①). Then, the inner HA core chains continuously absorbed water and swelled, enlarging the positively charged MMt-BH-HA/CS-ED NPs which would make them gradually sink into the negatively charged mucin mesh and glycocalyx structures of the tear film (step ②). Next, continuous water absorption and swelling of the inner core ultimately breaks the outer ED shell, exposing the negatively charged inner core MMt-BH-HA/CS NPs (step ③). This transition from the original positively charged to the new negatively charged stage (step ⑥) would change the interaction with the negatively charged mucin structure from the original opposite-charge attraction to repulsion, thus freeing the MMt-BH-HA/CS NPs from mucin meshwork. Finally, water and swelling would expose HA and CS chains (step ④), with NPs further sinking to the corneal epithelial surface and targeting corneal epithelial CD44 receptors due to interaction with the HA chains (step ⑤), thus further prolonging NPs retention on the ocular surface.^{25,50} Fundamentally, these micro-interactions (steps ②③④⑤) changed NPs elimination with tear flow into mucin turnover, ultimately prolonging the precorneal retention of the formulation and achieving a more sustained IOP-lowering effect.

Overall, the results of *in vivo* experiments revealed that MMt-HA/CS-ED NPs had longer precorneal retention to maintain higher drug concentrations in the tear fluid, resulting in more sustained IOP-lowering effect. MMt-HA/CS-ED NPs were significantly more effective than BH solution in lowering IOP, meeting the demand for long-term stable IOP control.

Conclusion

In this study, we developed a multifunctional nano-delivery system (MMt-BH-HA/CS-ED NPs) for ocular delivery to improve precorneal retention and thus increase drug bioavailability. The highly hydrophilic BH loading by a simple ionic cross-linking method would result in low encapsulation rates and drug leakage. In the current work, high encapsulation efficacy and drug loading were achieved by coating the ED shell, enhancing sustained release and reducing the initial burst release. Typically, eye drops are lost substantially due to rapid tear water turnover. Therefore, the prepared MMt-BH-HA/CS-ED NPs with high viscosity at low shear and long spread time resulted in prolonged precorneal retention of the NPs, enabling more time for micro-interactions to occur in the tear film. The potential micro-interactions between the formulation and the tear film may offer an explanation for sustained IOP-lowering effect of the NPs by shifting the drug clearance from being controlled by aqueous tear fluid turnover to being controlled by mucin turnover. This shift in drug clearance presents a good idea for the design of ocular or other mucosal drug delivery systems. In conclusion, multifunctional MMt-BH-HA/CS-ED NPs can synergistically lower IOP in a sustained manner, offering great potential in the treatment of glaucoma. The impact of physicochemical characteristics like particle size and surface charge of particles on the interaction with ocular surface mucins may be more intriguing to investigate in the future while concentrating on increasing anterior corneal retention.

Acknowledgments

This work was financially supported by the National Natural Science Foundation of China (No. 51192052) and the Science and Technology Planning Program of Guangdong Province, China (No. 2020B1212060055). We thank the Guangdong Provincial Engineering Center of Local Precision Drug Delivery System for help with the experiments.

Disclosure

The authors report no conflicts of interest in this work.

References

1. Almasieh M, Wilson AM, Morquette B, Cueva Vargas JL, Di Polo A. The molecular basis of retinal ganglion cell death in glaucoma. *Prog Retin Eye Res.* 2012;31(2):152–181. doi:10.1016/j.preteyeres.2011.11.002
2. Sacca SC, Izzotti A, Rossi P, Traverso C. Glaucomatous outflow pathway and oxidative stress. *Exp Eye Res.* 2007;84(3):389–399. doi:10.1016/j.exer.2006.10.008
3. Yadav KS, Rajpurohit R, Sharma S. Glaucoma: current treatment and impact of advanced drug delivery systems. *Life Sci.* 2019;221:362–376. doi:10.1016/j.lfs.2019.02.029
4. Rahic O, Tucak A, Omerovic N, et al. Novel drug delivery systems fighting glaucoma: formulation obstacles and solutions. *Pharmaceutics.* 2020;13(1):28. doi:10.3390/pharmaceutics13010028
5. Nemesure B, Honkanen R, Hennis A, et al. Incident open-angle glaucoma and intraocular pressure. *Ophthalmology.* 2007;114(10):1810–1815. doi:10.1016/j.ophtha.2007.04.003
6. Iezhitsa I, Agarwal R. New solutions for old challenges in glaucoma treatment: is taurine an option to consider? *Neural Regen Res.* 2021;16(5):967–971. doi:10.4103/1673-5374.297059
7. Burr J, Vale L. In Glaucoma. 2015:509–513.
8. Grieshaber MC, Flammer J. Is the medication used to achieve the target intraocular pressure in glaucoma therapy of relevance?--an exemplary analysis on the basis of two beta-blockers. *Prog Retin Eye Res.* 2010;29(1):79–93. doi:10.1016/j.preteyeres.2009.08.002
9. Baptiste DC, Hartwick ATE, Jollimore CAB, et al. Comparison of the neuroprotective effects of adrenoceptor drugs in retinal cell culture and intact retina. *Invest Ophthalmol Vis Sci.* 2002;43(8):120.
10. Awwad S, Mohamed Ahmed AHA, Sharma G, et al. Principles of pharmacology in the eye. *Br J Pharmacol.* 2017;174(23):4205–4223. doi:10.1111/bph.14024
11. Yellepeddi VK, Palakurthi S. Recent advances in topical ocular drug delivery. *J Ocul Pharmacol Ther.* 2016;32(2):67–82. doi:10.1089/jop.2015.0047
12. Jumelle C, Gholizadeh S, Annabi N, Dana R. Advances and limitations of drug delivery systems formulated as eye drops. *J Control Release.* 2020;321:1–22. doi:10.1016/j.jconrel.2020.01.057
13. Kimna C, Winkeljann B, Hoffmeister J, Lieleg O. Biopolymer-based nanoparticles with tunable mucoadhesivity efficiently deliver therapeutics across the corneal barrier. *Mater Sci Eng C Mater Biol Appl.* 2021;121:111890. doi:10.1016/j.msec.2021.111890
14. Rajurkar K, Dubey S, Gupta PP, John D, Chauhan L. Compliance to topical anti-glaucoma medications among patients at a tertiary hospital in North India. *J Curr Ophthalmol.* 2018;30(2):125–129. doi:10.1016/j.joco.2017.09.002
15. Ikuta Y, Aoyagi S, Tanaka Y, et al. Creation of nano eye-drops and effective drug delivery to the interior of the eye. *Sci Rep.* 2017;7:44229. doi:10.1038/srep44229
16. Nagai N, Yoshioka C, Mano Y, et al. A nanoparticle formulation of disulfiram prolongs corneal residence time of the drug and reduces intraocular pressure. *Exp Eye Res.* 2015;132:115–123. doi:10.1016/j.exer.2015.01.022
17. Khan N, Ameeruzzafar KK, Khanna K, et al. Chitosan coated PLGA nanoparticles amplify the ocular hypotensive effect of forskolin: statistical design, characterization and in vivo studies. *Int J Biol Macromol.* 2018;116:648–663. doi:10.1016/j.ijbiomac.2018.04.122
18. Kelly SJ, Hirani A, Shahidapury V, et al. A fibercept nanoformulation inhibits VEGF expression in ocular in vitro model: a preliminary report. *Biomedicines.* 2018;6(3). doi:10.3390/biomedicines6030092
19. Mehrandish S, Mirzaeei S. Design of novel nanoemulsion formulations for topical ocular delivery of itraconazole: development, characterization and in vitro bioassay. *Adv Pharm Bull.* 2022;12(1):93–101. doi:10.34172/apb.2022.009
20. Jain K, Kumar RS, Sood S, Dhyananadhan G. Betaxolol hydrochloride loaded chitosan nanoparticles for ocular delivery and their anti-glaucoma efficacy. *Curr Drug Deliv.* 2013;10(5):493–499. doi:10.2174/1567201811310050001
21. Abd-El salam WH, ElKasabgy NA. Mucoadhesive olaminosomes: a novel prolonged release nanocarrier of agomelatine for the treatment of ocular hypertension. *Int J Pharm.* 2019;560:235–245. doi:10.1016/j.ijpharm.2019.01.070
22. Huang G, Huang H. Application of hyaluronic acid as carriers in drug delivery. *Drug Deliv.* 2018;25(1):766–772. doi:10.1080/10717544.2018.1450910
23. Guter M, Breunig M. Hyaluronan as a promising excipient for ocular drug delivery. *Eur J Pharm Biopharm.* 2017;113:34–49. doi:10.1016/j.ejpb.2016.11.035
24. Zeng W, Li Q, Wan T, et al. Hyaluronic acid-coated niosomes facilitate tacrolimus ocular delivery: mucoadhesion, precorneal retention, aqueous humor pharmacokinetics, and transcorneal permeability. *Colloids Surf B Biointerfaces.* 2016;141:28–35. doi:10.1016/j.colsurfb.2016.01.014
25. Kim SJ, Owen SC. Hyaluronic acid binding to CD44S is indiscriminate of molecular weight. *Biochim Biophys Acta Biomembr.* 2020;1862(9):183348. doi:10.1016/j.bbmem.2020.183348
26. Mohammed MA, Syeda JTM, Wasan KM, Wasan EK. An overview of chitosan nanoparticles and its application in non-parenteral drug delivery. *Pharmaceutics.* 2017;9(4):53. doi:10.3390/pharmaceutics9040053
27. Mu M, Liang X, Chuan D, et al. Chitosan coated pH-responsive metal-polyphenol delivery platform for melanoma chemotherapy. *Carbohydr Polym.* 2021;264:118000. doi:10.1016/j.carbpol.2021.118000

28. Liang J, Yan H, Puligundla P, et al. Applications of chitosan nanoparticles to enhance absorption and bioavailability of tea polyphenols: a review. *Food Hydrocoll.* 2017;69:286–292. doi:10.1016/j.foodhyd.2017.01.041
29. Silva B, Marto J, Braz BS, et al. New nanoparticles for topical ocular delivery of erythropoietin. *Int J Pharm.* 2020;576:119020. doi:10.1016/j.ijpharm.2020.119020
30. Wu L, Lv G, Liu M, Wang D. Drug release material hosted by natural montmorillonite with proper modification. *Appl Clay Sci.* 2017;148:123–130. doi:10.1016/j.clay.2017.07.034
31. Baig MS, Ahad A, Aslam M, et al. Application of Box-Behnken design for preparation of levofloxacin-loaded stearic acid solid lipid nanoparticles for ocular delivery: optimization, in vitro release, ocular tolerance, and antibacterial activity. *Int J Biol Macromol.* 2016;85:258–270. doi:10.1016/j.ijbiomac.2015.12.077
32. Zhao Y, Li J, Han X, et al. Dual controlled release effect of montmorillonite loaded polymer nanoparticles for ophthalmic drug delivery. *Appl Clay Sci.* 2019;180:105167. doi:10.1016/j.clay.2019.105167
33. Park JH, Shin HJ, Kim MH, et al. Application of montmorillonite in bentonite as a pharmaceutical excipient in drug delivery systems. *J Pharm Investig.* 2016;46(4):363–375. doi:10.1007/s40005-016-0258-8
34. Thakral S, Thakral NK, Majumdar DK. Eudragit (R): a technology evaluation. *Expert Opin Drug Deliv.* 2013;10(1):131–149. doi:10.1517/17425247.2013.736962
35. Argu'eso IK. Role of mucins in the function of the corneal and conjunctival epithelia. *Int Rev Cytol.* 2003;231:1–49. doi:10.1016/S0074-7696(03)31001-0
36. Han X, Zhao Y, Liu H, et al. Micro-interaction of mucin tear film interface with particles: the inconsistency of pharmacodynamics and precorneal retention of ion-exchange, functionalized, Mt-embedded nano- and microparticles. *Colloids Surf B Biointerfaces.* 2021;197:111355. doi:10.1016/j.colsurfb.2020.111355
37. Hou D, Hu S, Huang Y, et al. Preparation and in vitro study of lipid nanoparticles encapsulating drug loaded montmorillonite for ocular delivery. *Appl Clay Sci.* 2016;119:277–283. doi:10.1016/j.clay.2015.10.028
38. Liu D, Wu Q, Chen W, et al. A novel FK506 loaded nanomicelles consisting of amino-terminated poly(ethylene glycol)-block-poly(D,L)-lactic acid and hydroxypropyl methylcellulose for ocular drug delivery. *Int J Pharm.* 2019;562:1–10. doi:10.1016/j.ijpharm.2019.03.022
39. Jin Q, Li H, Jin Z, et al. TPGS modified nanoliposomes as an effective ocular delivery system to treat glaucoma. *Int J Pharm.* 2018;553(1–2):21–28. doi:10.1016/j.ijpharm.2018.10.033
40. Liu H, Bi X, Wu Y, et al. Cationic self-assembled peptide-based molecular hydrogels for extended ocular drug delivery. *Acta Biomater.* 2021;131:162–171. doi:10.1016/j.actbio.2021.06.027
41. Xu T, Zhang J, Chi H, Cao F. Multifunctional properties of organic-inorganic hybrid nanocomposites based on chitosan derivatives and layered double hydroxides for ocular drug delivery. *Acta Biomater.* 2016;36:152–163. doi:10.1016/j.actbio.2016.02.041
42. Huang W, Zhang N, Hua H, et al. Preparation, pharmacokinetics and pharmacodynamics of ophthalmic thermosensitive in situ hydrogel of betaxolol hydrochloride. *Biomed Pharmacother.* 2016;83:107–113. doi:10.1016/j.biopha.2016.06.024
43. Willcox MDP, Argueso P, Georgiev GA, et al. TFOS DEWS II tear film report. *Ocul Surf.* 2017;15(3):366–403. doi:10.1016/j.jtos.2017.03.006
44. Li J, Tian S, Tao Q, et al. Montmorillonite/chitosan nanoparticles as a novel controlled-release topical ophthalmic delivery system for the treatment of glaucoma. *Int J Nanomedicine.* 2018;13:3975–3987. doi:10.2147/IJN.S162306
45. Natesan S, Pandian S, Ponnusamy C, et al. Co-encapsulated resveratrol and quercetin in chitosan and peg modified chitosan nanoparticles: for efficient intra ocular pressure reduction. *Int J Biol Macromol.* 2017;104(Pt B):1837–1845. doi:10.1016/j.ijbiomac.2017.04.117
46. Vaculikova L, Plevova E, Ritz M. Characterization of montmorillonites by infrared and raman spectroscopy for preparation of polymer-clay nanocomposites. *J Nanosci Nanotechnol.* 2019;19(5):2775–2781. doi:10.1166/jnn.2019.15877
47. Paradkar MU, Parmar M. Formulation development and evaluation of Natamycin niosomal in-situ gel for ophthalmic drug delivery. *J Drug Deliv Sci Technol.* 2017;39:113–122. doi:10.1016/j.jddst.2017.03.005
48. Kalam MA. Development of chitosan nanoparticles coated with hyaluronic acid for topical ocular delivery of dexamethasone. *Int J Biol Macromol.* 2016;89:127–136. doi:10.1016/j.ijbiomac.2016.04.070
49. Bi YG, Lin ZT, Deng ST. Fabrication and characterization of hydroxyapatite/sodium alginate/chitosan composite microspheres for drug delivery and bone tissue engineering. *Mater Sci Eng C Mater Biol Appl.* 2019;100:576–583. doi:10.1016/j.msec.2019.03.040
50. Liu D, Lian Y, Fang Q, et al. Hyaluronic-acid-modified lipid-polymer hybrid nanoparticles as an efficient ocular delivery platform for moxifloxacin hydrochloride. *Int J Biol Macromol.* 2018;116:1026–1036. doi:10.1016/j.ijbiomac.2018.05.113
51. Liu H, Han X, Li H, et al. Wettability and contact angle affect precorneal retention and pharmacodynamic behavior of microspheres. *Drug Deliv.* 2021;28(1):2011–2023. doi:10.1080/10717544.2021.1981493